

Design and Development of a Modular, Multichannel Photoplethysmography System

Karthik Budidha[✉], Victor Rybynok, and Panayiotis A. Kyriacou, *Senior Member, IEEE*

Abstract—In this paper, we present the design, development, and validation of a ‘modular photoplethysmography (PPG) system called ZenPPG. This portable, dual-channel system has the capability to produce “raw” PPG signals at two different wavelengths using commercial and/or custom-made PPG sensors. The system consists of five modules, each consisting of circuitry required to perform specific tasks, and are all interconnected by a system bus. The ZenPPG system also facilitates the acquisition of other physiological signals on-demand including electrocardiogram (ECG), respiration, and temperature signals. This report describes the technical details and the evaluation of the ZenPPG along with results from a pilot *in vivo* study on healthy volunteers. The results from the technical evaluations demonstrate the superiority and flexibility of the system. Also, the systems’ compatibility with commercial pulse oximetry sensors such as the Masimo reusable sensors was demonstrated, where good quality raw PPG signals were recorded with the signal-to-noise ratio (SNR) of 50.65 dB. The estimated arterial oxygen saturation (SpO₂) values from the system were also in close agreement with commercial pulse oximeters, although the accuracy of the reported SpO₂ value is dependent on the calibration function used. Future work is targeted toward the development of variations of each module, including the laser driver and fiber optic module, onboard data acquisition and signal processing modules. The availability of this system will help researchers from a wide range of disciplines to customize and integrate the ZenPPG system to their research needs and will most definitely enhance research in related fields.

Index Terms—Electrocardiogram, modularity, optoelectronics, oxygen saturation, photoplethysmography (PPG), physiological monitoring, pulse oximetry, raw PPG signals.

I. INTRODUCTION

THE introduction of photoplethysmography (PPG) by Hertzman and Speelman [1] in the 1930s was one of the major steps in exploring the interactions between optical radiation and the skin. The principle of operation of the PPG is based on the assumption that light is attenuated when it is shone on vascular tissue and the attenuation shows variations depending on the volume of blood entering the tissue under observation [2]. A monochromatic light source

such as laser or light emitting diode (LED) is normally used to shine light through the tissue, while the attenuations in light intensity are detected by a photodetector. The wavelength of the light source used depends on the type of blood volume changes under observation (i.e., oxygenated or deoxygenated). The detected PPG signal consists of a steady component (DC), which is related to the relative vascularization of the tissue, and a pulsatile component (AC), which is related to changing blood volume [2].

Although the PPG technology has been in use for over 80 years, it is the successful commercialization of the pulse oximeters in the 1980s and the subsequent advancements in signal processing algorithms that have brought about renewed interest on the PPG among researchers [3]. In particular since its potential use as a diagnostic tool for measuring physiological variables beyond arterial oxygen saturation and heart rate (HR), such as venous oxygen saturation [4], pulse rate variability [5], pulse wave velocity (PWV) [6], blood pressure [7], and pulse transit time (PTT) [8] has been demonstrated. These newly derived variables are now being used as diagnostic markers for conditions such as arterial stiffness [9], hypertension, peripheral vascular disease [10], stress, endothelial dysfunction [11], and haemorrhology [12]. Furthermore, PPG has generated immense interest in the development of unique sensor technology utilizing either miniaturized optoelectronic components or optical fibers, to measure the volumetric changes directly from organs such as the esophagus [13], liver, bowel [14], brain [15], ear canal [10], and other vascular tissues such as free flaps [16]. In the last few years, PPG has also found its place in the remote health monitoring market. Manufacturers and researchers are integrating the existing PPG technology into everyday wearable devices such as wrist watches, earphones, and rings, and are offering a way to continuously monitor cardiac health [17], [18].

Progress in these areas is, however, dependent on ability to the PPG processing system to record good quality raw PPG signals, from multiple channels, ideally at more than one wavelength, for real-time or retrospective analysis. Although commercial monitors that offer multichannel acquisition exist, most of these monitors only output one wavelength, amplitude modulated, phase modulated and postprocessed signals. The postprocessing and amplitude modulation of the PPG signal in these systems causes the suppression of PPG signal features, leading to a loss of valuable physiological information [19]. For instance, feature extraction to measure venous saturation or biometric recognition is not possible from

Manuscript received September 18, 2017; revised November 2, 2017; accepted January 3, 2018. The Associate Editor coordinating the review process was Dr. Domenico Grimaldi. (*Corresponding author: Karthik Budidha.*)

The authors are with the Research Centre for Biomedical Engineering, School of Mathematics, Computer Sciences & Engineering, City, University of London, London EC1V 0HB, U.K. (e-mail: karthik.budidha.1@city.ac.uk).

Color versions of one or more of the figures in this paper are available online at <http://ieeexplore.ieee.org>.

Digital Object Identifier 10.1109/TIM.2018.2810643

PPGs acquired from these devices. It is also meticulous to concurrently control and acquire PPG signals from multiple pulse oximeters along with other physiological signals such as ECG, the respiration signal, that are commonly required for calculating some of the diagnostic variables mentioned earlier. Phase differences between these measurement systems can also be a major concern while analyzing the acquired data since all the acquired signals will be out of phase with respect to each other to a certain degree.

Hence, in the absence of a multiwavelength PPG system that can produce raw PPG signals and other physiological signals on-demand, researchers have resolved in custom building their own research systems. One of the many examples of such systems is the Ultra-Low-Power Sensor Evaluation Kit developed by Tobola *et al.* [20] to measure ECG, respiration, motion, body temperature, and PPG. Other examples of such systems include [21]–[23]. The demand for raw PPG signals has also prompted manufacturers to develop integrated analog front-end chips such as the AFE4490 and MAX30100 [24], [25]. However, none of the integrated solutions or the research systems developed to date offer a modular, simple-to-use, multiwavelength and multichannel PPG acquisition system, that is flexible and adaptable to the needs of the large PPG research community. Therefore, there is an unmet need for a multichannel research system that allows simultaneous acquisition of raw PPGs to carry out fundamental investigations using PPG. Such investigations can include bilateral PPG acquisition for diagnosis of lower limb peripheral arterial disease, or for investigating the differences between peripheral and central perfusion.

Hence, we designed and developed “ZenPPG”—a modular PPG research system, which combines the advantages of standardization of instrumentation, compatibility with commercial sensors, and ability to interchange independent modules to customize the system for specific projects. In this paper, we introduce the design and development of the proposed system in detail and provide a preliminary assessment of its performance.

II. METHODS

The design of the system is based on previous instrumentation developed by the Research Center for Biomedical Engineering, at City, University of London, London, U.K. The system is designed to satisfy the following requirements.

- 1) The design of the system should be modular and allow for incremental improvements so that further improvement of any single module will “not” affect the performance or the architecture of other modules.
- 2) The system should be portable in size, and contain a minimum of two PPG channels, with each channel capable of generating PPG signals at least two wavelengths.
- 3) The system should accommodate an ECG amplifier with standard 3-lead or 5-lead connector so that the ECG signal can be used as a timing reference for the PPG signals.
- 4) The system should output “raw” PPG (AC and DC) and ECG signals with no amplitude or phase modulations.

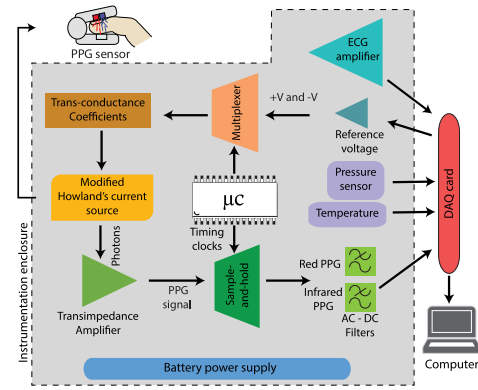


Fig. 1. Top-level architecture of ZenPPG system.

- 5) The system should operate with both custom built PPG probes and standard commercial pulse oximeter probes.
- 6) The system should be easy to use and run on both batteries and a power supply.
- 7) To keep the system cost effective, all the mechanical and electrical components used in the system should be standard industrial components. The system should comply with the U.K. medical device technical standard ISO 60601.

Taking the above-mentioned requirements into consideration, the “ZenPPG” system was developed. The current version of the system accommodates two dual-wavelength PPG channels along with an ECG amplifier, thermocouple amplifier, and an airflow pressure sensor.

A. Electrical Design of ZenPPG

The block diagram shown in Fig. 1 gives the top level architecture of the “ZenPPG” system. The electrical and design characteristics of both the PPG channels in the system are identical. Both the emitters in each channel are driven by a constant emitter driver which consists of three parts: a reference control voltage (RCV) circuit, a multiplexer, and a modified Howland current source (MHCS). The reference voltage circuit generates the constant voltage required to drive the LEDs. The multiplexer is to generate a timed switching signal used to turn on the LEDs alternatively. The LEDs are switched ON alternatively in order to allow for the independent sampling of light at different wavelengths by the photodetector. An MHCS is then used to convert the switching voltage signal into the current that is used to turn the LEDs in the probe “ON” and “OFF.”

The reflected or transmitted light photons from the vascular tissue are then detected by the photodetector, which generates a current proportional to the incident light power. This current is then converted into a voltage signal consisting of components detected at different wavelengths by the transimpedance amplifier (TIA). A sample-and-hold amplifier (SHA) then separates the mixed output from the TIA into individual wavelength fragments (PPG signals). A programmable microcontroller is used to control the LED switching and

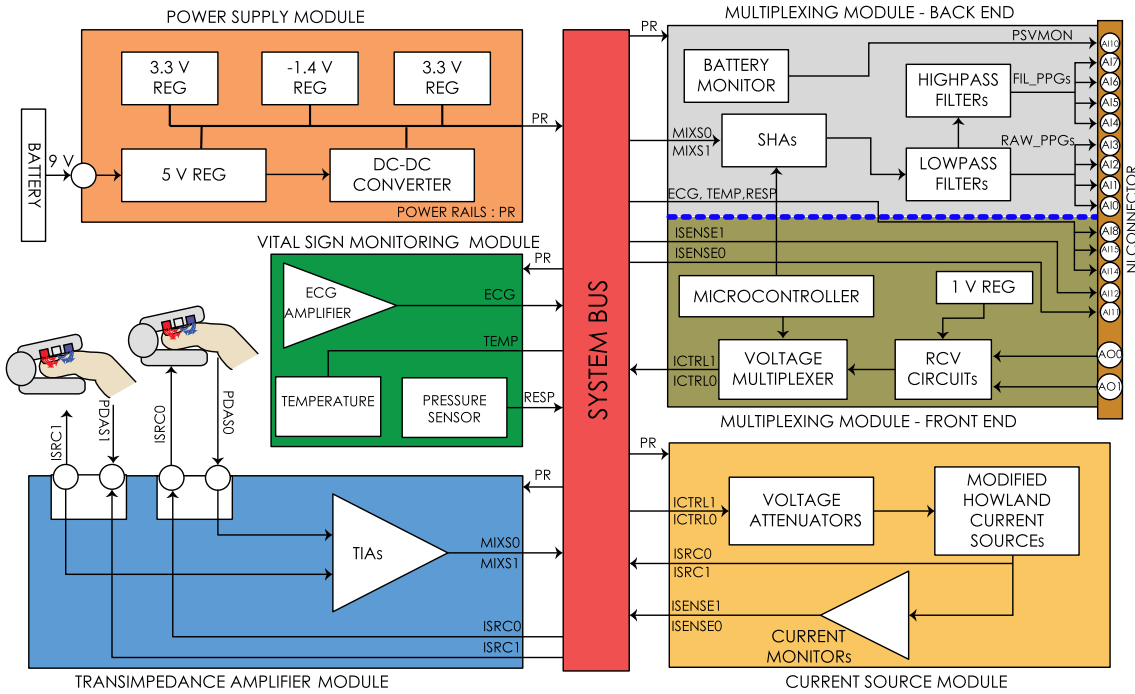


Fig. 2. Detailed block diagram showing the architecture of ZenPPG.

demultiplexing of the signals. The individual PPG signals are then low-pass filtered to remove the high-frequency switching noise. The AC component of the PPG signals is extracted by high-pass filtering the raw PPG signals. The system also hosts an ECG amplifier to detect the QRS complex of the ECG signal, an airflow pressure sensor that can be used to measure respiration rate and a thermocouple amplifier used to measure skin temperature. The raw AC and DC PPG signals, the ECG, respiration, and temperature signals are digitized by a National Instruments data acquisition (DAQ) card (National Instrument Corporation, Texas, USA) and are displayed and stored on the PC or laptop.

The circuitry of the entire system is split into five individual modules which are interconnected by a double-sided system bus. Each individual module has a specific function in acquiring and processing various signals. The PPG modules are the TIA module, the CS module, and the multiplexing module. The other two modules are the power supply conditioning module and the vital sign monitoring module. A detailed block diagram showing the architecture of the ZenPPG is shown in Fig. 2. Sections II-A1–II-A7 describe the design of each module in detail.

1) *System Bus*: To make the system modular and reusable, a system bus was designed, which interconnects all other modules together. The system bus consists of six (three on each side) receptacle 50-way surface mount connectors (SAMTEC, Indiana, USA). It is designed in a way that every single pin in a given connector corresponds to the same pin in all other connectors. Since all the 50 pins on every connector are the same, it provides a medium of interaction between various modules. All other modules are all furnished with gold plated, through-hole, right angle 50-way headers that connect to the bus. Each pin in the system bus is assigned to a particular

net, hence making it the only module in the system that is inflexible or unalterable.

2) *Power Supply Module*: The ZenPPG system runs on two standard 9-V PP3 batteries encased within the portable system case or on 5-V universal serial bus (USB) supply. The batteries used were rechargeable Li-ion batteries with a capacity of 650 mAh (Superex Technologyco.LTD, Wanchai, Hongkong). The power supply conditioning module consists of the circuitry required to regulate the main battery or USB power supply into multiple DC power rails. This is to reduce power consumption, provide operational stability, and improve system efficiency.

The initial DC power supply from either the USB (5 V) or the batteries (9 V) is regulated down to +5 and −5 V using an isolated point-of-load DC–DC converter (IA0505D, XP power, Singapore). These +5 V and −5 V supplies are used to power microchips in the CS module, the vital sign module and the multiplexers in the multiplexing module. All other analog microchips run on +3.3 V and −1.4 V supplies. The +3.3 V supply is generated using a linear low dropout voltage regulator (MCP1703T, Microchip Technology, Arizona, USA), while the −1.4-V supply is generated using a low drop-out negative micropower regulator (LT1964ES5, Linear Technology, California, USA). A separate +3.3 V supply is generated using a linear low dropout voltage regulator (MCP1703T, Microchip Technology, Arizona, USA), and is used to power digital microchips such as the microcontroller. Digital circuitry usually draws large currents from its supply during switching and is very noisy. On the other hand, analog circuitry is quite vulnerable to noise on both supply rails and grounds. Thus, to prevent digital noise from corrupting analog performance, separate power rails and ground returns were implemented in the system.

3) *Multiplexing Module–Front End*: The multiplexing module is the “heart” of the PPG processing system. The circuitry within the multiplexing board can be divided into two parts, the front-end and the back-end. The front-end consists of the circuitry required for emitter driver control, and the back-end consists of demultiplexers and filters. As mentioned earlier, the emitter driver consists of three main parts: a RCV circuit, a voltage multiplexing circuit, and an MHCS. The front end of the multiplexing board hosts both the RCV circuit and the multiplexing circuit. These circuits were designed by keeping two main specifications in mind.

- 1) Each LED has to be able to switch ON and OFF at a frequency of at least 100 Hz, as it is sufficient to sample the PPG signal.
- 2) Each LED “on time” should be sufficient to obtain an undistorted light intensity sample.

a) *Reference control voltage (RCV) circuit*: The purpose of the RCV circuit is to provide independent control over LED currents on both channels. Each LED in both PPG channels is controlled by an individual RCV circuit. The design of all four RCV circuits is similar and consists of a DC reference voltage source and a voltage attenuator. The reference voltage (V_{Ref}) on channel-1 is generated by the analog output ports AO0 and AO1 of a 16-bit NI DAQ card (National Instrument Corporation, Texas, USA). The analog output ports of the DAQ card can drive the LED CS with a resolution of $305 \mu V$. In the current setup, AO0 is configured to generate a voltage between -5 and 0 V. Port AO1 is configured to generate a voltage between 0 and 5 V. On channel-2, V_{Ref} is generated using a low noise drop-out 1 V regulator (LM4140ACM, Texas Instruments, Texas, USA). The output ranges of AO0 and AO1 were then attenuated down to -1 to 0 V and 0 to 1 V using the voltage attenuator circuit, which is a voltage divider with an op-amp buffer that divides the input voltage by five.

V_{Ref} on channel-2 is by a constant onboard 1 -V regulator. The 1 -V output from the voltage regulator is attenuated to -1 to 0 V and 0 to 1 V using the attenuator circuits. This configuration allows for digital control of LEDs on channel-1 and analog control of LEDs using trimmers on the other. Digital control of LEDs on both channels is not possible in this design due to the limited number of output channels on the DAQ card.

b) *Voltage multiplexing circuit*: The purpose of the multiplexing circuit is to generate a timed switching signal used to turn on both the LEDs alternatively. The LEDs are switched ON alternatively in order to allow the independent sampling of light at each wavelength by the photodetector. Switching is attained by connecting the positive and the negative voltages from the RCV circuits to a double-pole 4–throw (DP4T) analog multiplexer (MC14052BD, ON Semiconductor, Arizona, USA). The multiplexer selects one of the two input voltage signals (either positive or negative) and outputs the selected input into a single line, producing two switching signal varying between $+1$ V and -1 V. The data select lines determine which input is passed on to the output. The data select lines are timed clocks generated by an 8-bit Atmel ATtiny 2313-20SU microcontroller unit (MCU) (Atmel Corp, California, USA) at a frequency of 800 Hz from the

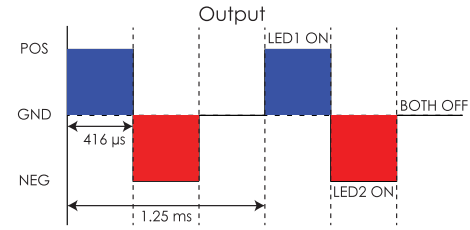


Fig. 3. One of the outputs of the dual- 4 channel multiplexer. LED1 is first switched ON for $416 \mu s$, followed by the LED2, and then an off period, where both LEDs are off.

port-D of the MCU. When the output of the multiplexer is positive, one of the LEDs is switched “ON,” and when negative, the other LED is switched “ON.” Both the LEDs are off when the voltage is at zero. The duty cycle time (t) of each LED is

$$t = \frac{1}{f} \times d = 416 \mu s$$

$$\text{where } d = \frac{\text{Time the signal is active}}{\text{Total period of the signal}} \times 100\%. \quad (1)$$

Each emitter is, hence, switched “ON” every 1.25 ms for a duration of $416 \mu s$. Fig. 3 shows one of the multiplexers out signals. The two outputs of the multiplexer are passed through the system bus into the CS module, where the voltage is converted into current required to power the LEDs.

4) *Current Source Module*: The CS module consists of two identical current driver circuits that are used to drive the LEDs on both the channels. The module also consists of two current monitoring circuits, which are used to continuously monitor the current through the LEDs. The current driver circuit used is a linear, unity gain MHCS. MHCS was used as it avoids the “floating common point” issues usually experienced by other CSs such as the H-bridge or transistor-based switching CSs, and also as it offers high output impedance [26]. The accuracy of the MHCS is, however, determined by the choice of the amplifier and the matched resistors. Hence, a precision op-amp (AD8672, Analog Devices, Massachusetts, USA) with low input bias current (14 nA) and offset voltage ($70 \mu V$) was used. Also, a high precision (0.1%) resistor array was used in the current driver design.

The bidirectional switching outputs of the multiplexer (max: ± 1) from the multiplexing module are first attenuated down to a maximum of ± 100 mV before passing it to the current driver. This is to limit the maximum current to the LEDs to 100 mA. In applications where high power is required for instance to drive laser diodes, the multiplexer output can be connected directly to the current driver allowing to drive the laser diodes up to 1 A. The current output of the MHCS is then passed through the system bus into the LEDs in the connected probe.

Two disincentive features of the CS module are as follows.

- 1) The current limiters which only allow a maximum current of ± 100 mA to pass through the LEDs, even in the event of a malfunction (when the input voltage to the CS exceeds 100 mV), preventing any damage to the sensors.

- 2) The current monitors to precisely measure the current across each LED, providing feedback to control the LED currents.

The current through the LEDs was limited to ± 100 mA using a fast power push-pull (NPN-PNP) transistor switch (PMD3001D, NXP Semiconductors, Eindhoven, Netherlands) between the Howland CS op-amp output and the LEDs. The current through the LEDs was monitored by inputting voltage across the load resistor and the current through the load resistor as differential inputs to the instrumentation amplifier. The instrumentation amplifier produces an output voltage equivalent to the current across the LEDs, which is passed through the bus into the multiplexing board and into the DAQ card for acquisition.

5) *Transimpedance Amplifier (TIA) Module*: The TIA module consists of two identical TIAs that convert the light photons detected by the photodetector into a mixed voltage signal. This voltage signal contains photometric information from both wavelengths. A zero bias topology was used in TIA design as linearity to light intensity is of paramount importance in PPG applications and the multiplexing frequency is not high enough (only 800 Hz) to use the reverse bias topology. Also, since zero biased circuit produces low noise, the detection of small amplitude PPG becomes easily possible.

However, in an intermediate gain application (100 k to 1 M) such as in pulse oximetry, the TIA bandwidth is restricted by the op-amp bandwidth, the phase compensation and the large parasitic capacitance of the photodiode. Hence, while designing TIA for the ZenPPG system, opamps (OPA380, Texas Instruments, Texas, USA) with large bandwidth (90 MHz) and open-loop gain (130 dB) were used, and a phase compensation capacitor in the order of few picofarads is integrated in the TIA circuit to provide stability to the circuit. The -3 -dB frequency and the open-loop gain bandwidth of the TIA circuit used was 58.9 and 142 kHz (at TIA gain of 270 K). The module also hosts two female DB9 connectors for interfacing with the PPG probes. The connector and the pinout of the connector used are similar to commercial pulse oximeter probes. Hence, giving the flexibility to use most commercial PPG probes without any additional requirements.

6) *Multiplexing Module-Back End*: The back end of the multiplexing module consists of a microcontroller to generate timing signals that control the multiplexers, an SHA to separate the mixed PPG signals from the TIAs into two independent PPG signals containing information at specified wavelengths, and filters to precondition the PPG signals before digitization.

a) *Microcontroller unit (MCU)*: An Atmel ATtiny 2313A-20SU (Atmel Corp, CA, USA) micro-controller was used as a master clock and timing generator. The ATtiny 2313A-20SU is an 8-bit MCU with 18-programmable I/O lines and a maximum operating frequency of 20 MHz. As mentioned earlier, the port-D of the MCU is used to generate two clocks for multiplexing the LEDs. Port-B of the MCU is programmed to output another three clocks used for synchronizing the SHA that separated the mixed PPG signals into independent wavelength components. The clocks from port-B

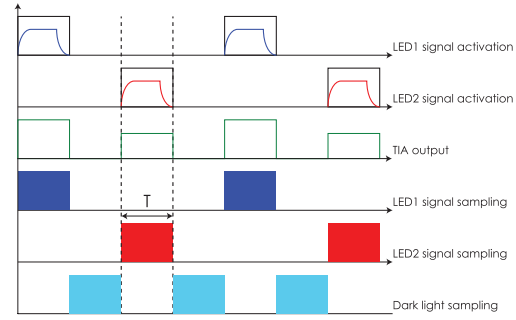


Fig. 4. PPG signal sampling at two different wavelengths using time windowing.

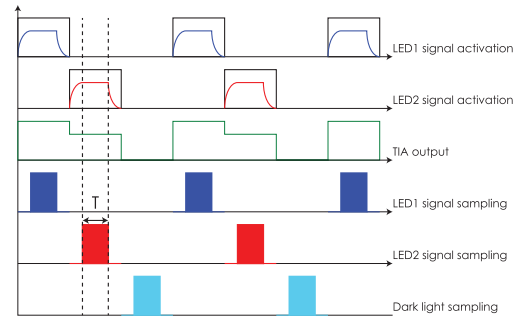


Fig. 5. Time windowing solution for avoiding switching noise, by sampling at the plateau of the LED on time.

were in sync with the clocks from port-D, as mistiming would lead to an inappropriate sampling of PPG signals.

b) *Time-multiplexing for PPG signal sampling*: As mentioned earlier, the photons detected by the photodetector in a PPG probe are continuously recorded as a voltage signal using the TIA. The direct sampling and digitization of this signal are possible when the photodiode sees just one light source. In which case the signal can simply be sampled at the Nyquist rate. However, when there are two or more light sources, the photodetector “cannot” distinguish between parts of the light power received from different light sources. To overcome this limitation time windowing is used. An example of a two channel time windowing sequence usually used in pulse oximeters is shown in Fig. 4. Although the timing diagram might seem very straightforward, in practice the signal is not as clean as it is in Fig. 4. Numerous high-frequency distortions are mixed together with the useful PPG signal. When a light source such as an LED is switched from an “OFF” to “ON” state and vice versa, there is a slight delay between the transitions, usually referred to as the transient response of a diode. During these transition states, the intensity of the light detected does not represent the true light level. Therefore, by sampling the PPG signals during the entire LED activation period as in Fig. 4, the switching noise is also sampled.

To overcome this problem, a new schema commonly used in telecommunications was implemented in the “ZenPPG” system. In this new approach, a slight time delay is introduced between the switching of the emitters and the triggering of the demultiplexer sampling circuit. In this way, the photodetector output is sampled from the middle of the “plateau” region of the signal as shown in Fig. 5. This ensures that the

detection circuit has enough time to settle before sampling. Thus, producing an output signal that is more representative of the true light level. However, this schema requires the light source activation time window to be sufficiently long so that a proper sample can be acquired. Long light source activation windows mean low multiplexing rate and reduced number of optical channels. But since the output is only sampled in the middle of the plateau region, there is no need to sample dark light after activation of each LED. Instead, dark light can be sampled once both the LEDs are activated. Thereby improving the sampling time and multiplexing rate. In the current system, the LEDs were multiplexed at 800 Hz.

c) Sample-and-Hold Amplifier (SHA): The mixed voltage signal from the TIA is split into two PPG signals, each containing photometric information from a specified wavelength using an SHA. The SHA adopted the time windowing schema shown in Fig. 5. The SHA circuit consisted of a switch (demultiplexer), an energy storage device (capacitor), and an output buffer. The demultiplexer used is a double-pole 4-throw (DP4T) analog demultiplexer (MC14052BD, ON Semiconductor, Arizona, USA). The data select lines are the clocks from Port-B of the MCU. When the mixed PPG signal is split into two different components, it is necessary to “hold” the sampled voltage until the next clock pulse triggers a new acquisition. Hence, a storage device, i.e., the capacitor, is used to hold the sampled voltage. In the sample mode, the voltage on the hold capacitor follows the specific input voltage. In the hold mode, the demultiplexer switch is open, and the capacitor retains the voltage present before it was disconnected from the demultiplexer. The output buffer offers a high impedance to the hold capacitor to keep the held voltage from discharging prematurely [27].

The performance of this circuit is mostly dependent on the switching frequency and the chosen capacitor value. If the value of the capacitor is too large then there is a corresponding increase in acquisition time and a reduction in bandwidth and slew rate. On the other hand, if the capacitor value is too small then the capacitor discharges quickly resulting in chopping effects and “saw” shaped modulations. The frequency of switching also needs to be sufficiently large as low switching speeds result in the circuit being open for extended times, during which the capacitor can retain some of its charge. Through a series of experiments, it was found that a 220-nF capacitor provides optimal performance in PPG applications and was used in the current system [28]. There are 4 SHA’s in the system to split the TIA output of each channel into two individual wavelength components.

d) Analog filters: The outputs of the SHAs were fed through individual antialiasing filters with a cut-off frequency of 80 Hz. This is to limit the bandwidth of the PPG signals and stop the high-frequency switching noise from corrupting the PPG signals. The design of the filter is a passive RC filter stage providing a low-frequency path to the input of an op-amp buffer. The filtered PPG signals are then passed onto the NI DAQ card for digitization and further analysis from the onboard 68-pin NI connector. These raw signals contain both AC and DC components, which can be separated digitally using digital filters. However, to increase the AC

resolution, the low-pass filtered PPG signals were also passed through a first-order active high-pass filter with a gain of 180. This ensured that the DC components were removed from the PPG signal and the AC signal was amplified nearly to the full range of the DAQ card. The AC PPG signals are also digitized by the NI DAQ card connected to the 68-pin NI connector on the back-end of the multiplexing module.

The back-end of the multiplexing module also consists of a battery monitoring circuit, which is a voltage divider that divides the 5 V main supply to 1 V. This 1 V signal is continuously sampled by the DAQ card, and displayed on the PC, hence giving the user an indication of the battery’s state of charge.

7) Vital Sign Monitoring Module: The vital sign monitoring module consists of an ECG channel, a skin temperature measurement channel, and a respiration measurement channel.

A Lead I ECG amplifier was developed for monitoring the QRS complex of the ECG signal, which can be used as a timing reference for the PPG signals. An instrumentation amplifier INA128 (Texas Instruments, Texas, USA) with high common-mode rejection ratio (120 dB) and a very high input impedance ($10^{10}\Omega$) was used to acquire the ECG signal. The ECG signal acquired from the instrumentation amplifier was bandpass filtered to remove the large DC offset and any other interference signals such as the 50 Hz mains interference. The bandpass filter used consists of a second-order Sallen-Key high-pass filter, to remove the DC component in the ECG signal, and a second-order Sallen-Key low-pass filter which attenuated high frequencies. The lower and upper cut-off frequencies of the bandpass filter are 0.37 and 36 Hz, respectively. The bandpass filter is of unity gain with both resistors and capacitors of the same value, giving it a quality factor (Q) of 0.51. Interfacing between the 3-lead ECG cable and the instrumentation is through the onboard 6-pin AAMI connector.

The module consists of a signal conditioned 40PC001B pressure sensor (Honeywell Inc, Illinois, USA) to measure airway pressure using either a mouthpiece or a breathing mask. The changes in pressure during respiration are detected by the pressure sensor as a voltage signal with a frequency equivalent to the respiration rate. Using this modulating pressure signal the respiration rate is calculated. The breathing mask is connected to the pressure sensor via an airway gas sampling line. This module also consists of a monolithic thermocouple amplifier with cold junction compensation, configured to measure skin temperature using a K-type thermocouple. Since the output of the thermocouple is nonlinear with respect to temperature, the thermocouple amplifier (AD595CQ, Analog Devices, Massachusetts, USA) was used to produce a linear voltage output with a sensitivity of 10 mV/°C. AD595CQ was gain trimmed to match the transfer characteristic of J and K type thermocouples. The interface between the k-type thermocouple and the amplifier is through the 2-pin, PCB mount thermocouple socket (IM-K-PCB, Labfacility, Twickenham, U.K.). The ECG, pressure, and temperature signals from this module are passed to the NI DAQ card via the back-end of the multiplexing module.

B. Mechanical Design of ZenPPG

As mentioned earlier, a modular design approach was implemented in the mechanical design of the ZenPPG system, whereby the entire system was split into subsystems which acted independently and were connected together through a bus interface. In addition to reusability, this approach provides efficient troubleshooting, since bugs can be traced to specific system modules.

The ZenPPG system was designed with the aid of 3-D CAD modeling software called SolidWorks 2014 (Dassault Systemes, SolidWorks Corp., Massachusetts, USA). The inclusion of 3-D modeling and electronic design automation in the design process has made it easier to recognize potential design flaws, better visualize how the modules interface with each other in the system and in reducing the number of revisions during manufacturing.

1) *Enclosure*: All six modules in the system along with a dual 9 V PP3 battery case were designed to fit inside a portable unit measuring $160 \times 103 \times 56$ mm. The portable enclosure was made of clear anodized aluminum (1455N1601, Hammond Manufacturing, Ontario, Canada). The rugged aluminum body consists of a slide removable belly plate and extruded internal slots that are used to mount the PCBs horizontally. The enclosure consists of two replaceable metal endplates which were milled in the laboratory to accommodate the connectors. An anodized aluminum body was used so that it can be connected to the ground plane, providing better shielding, reducing EMI, and minimize electrical shock hazard.

The front panel of the system incorporated two standard DE9 connectors, an AAMI ECG connector, a thermocouple connector and an inlet for connecting the gas sampling line to the pressure sensor. These connectors are used to connect the PPG probes, the ECG cable, and the thermocouple. The rear panel consists of an ON/OFF switch to control the system, an LED indicator, a 68-pin serial bus connector for interfacing with National Instruments DAQ card, and inlets to access the trimmers which can be used to control the LED currents. The rear panel also hosts the mini USB connector and the battery case which is used for powering the system. The photographs showing the front and back panels and the PCB assembly is shown in Fig. 6. The circuit diagrams and mechanical diagrams of the system are also provided as supplementary material.

2) *PCBs*: All the modules used in the processing system were designed using an electronic design automation software package known as Altium Designer (Altium Limited, Sydney, Australia) and were manufactured using a Computer Numeric Control machine (Bungard Elektronik GmbH & Co.KG, Windeck, Germany). The dimensions of all the modules were $100 \times 78.95 \times 1.6$ mm, except for the CS module and the system bus. The dimensions of the CS module and system bus are $100 \times 50 \times 1.6$ mm and $95 \times 47.6 \times 1.6$ mm, respectively. Double-sided copper clad boards of 1.6 mm thickness were used to manufacture the PCBs.

C. Data Acquisition

A DAQ system was developed which incorporated all the elements required for the hardware control and acquisition of

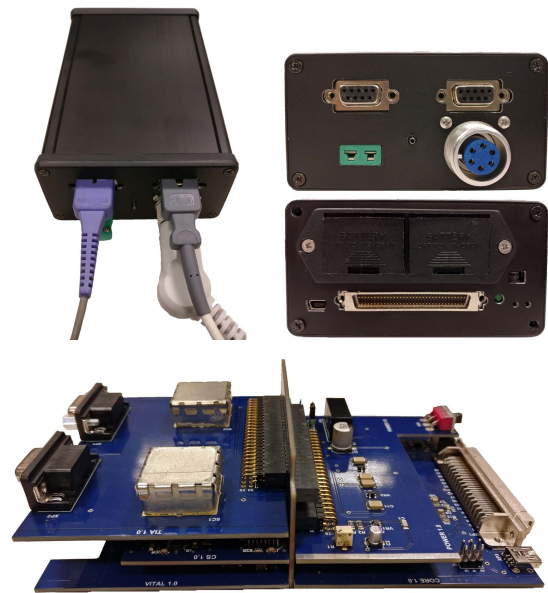


Fig. 6. Photographs showing the front and back panel of the ZenPPG system along with the PCB assembly.

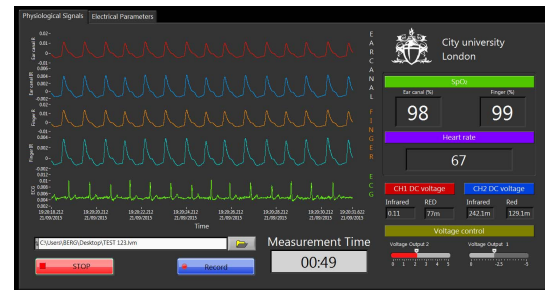


Fig. 7. Front panel of the virtual instrument (VI) showing the continuous display of AC PPG signals, the ECG signal (green). The SpO_2 values are also displayed on the right of the VI.

various signals from the ZenPPG. The DAQ system comprises a software program, or VI, implemented in LabVIEW and a DAQ card from National Instruments (National Instrument Corporation, Austin, Texas). The two main functions of the developed VI are: 1) digitization of signals from the ZenPPG and 2) controlling the emitter driver circuit. Other functions of the VI include recording and saving data, digital signal processing and estimation of various parameters such as HR, respiration rate and SpO_2 . The front panel of the VI as shown in Fig. 7 displays all the PPG, ECG, respiration, and temperature waveforms. All the parameters calculated from the PPG signals are also displayed on the front panel. The VI was designed to acquire all the signals at a sampling frequency of 1 kHz.

III. RESULTS

Following the design and fabrication of the ZenPPG system, the system's performance was evaluated by means of initial laboratory testing. The details of the testing conditions and the results obtained are described in this section.

A. Technical Evaluation

1) *Signal-to-Noise Ratio (SNR)*: First, the SNR of the PPG signals acquirable from the ZenPPG system was

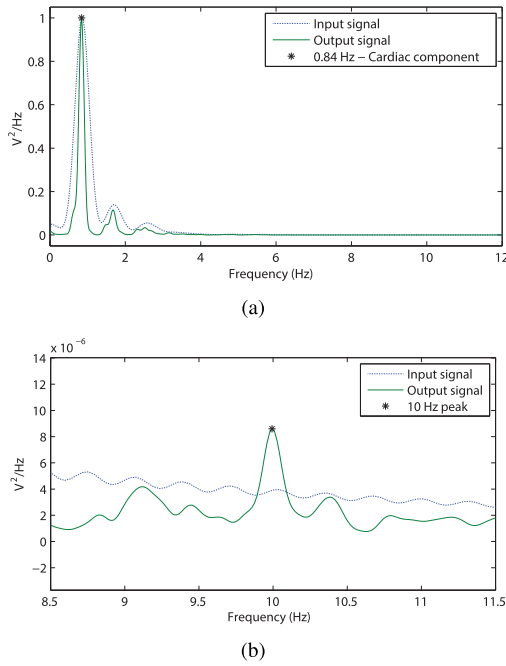


Fig. 8. Frequency spectrum of the input and the output PPG signals showing (a) cardiac and (b) noise components. The 10-Hz noise peak is used to calculate SNR.

measured experimentally. For this test, a function generator was programmed to output a prerecorded PPG signal with a frequency of 0.84 Hz. The output of the function generator was then used as the reference voltage to drive the LEDs in a commercial pulse oximeter probe connected to the channel-1 of the ZenPPG system. Since the reference voltage to the CS was continuously modulated in the shape of a PPG signal, the intensity of the LEDs in the probe will also modulate in a similar fashion. Provided that the light absorbance between the LEDs and the photodetector does not change during measurement, the output of the photodetector will also reflect the input reference signal. Hence, by comparing the input reference PPG signal with the output signals obtained from the ZenPPG in the frequency domain, the SNR can be calculated. A small block of clear silicon was used as the light absorber between the LEDs and the photodetector in this experiment. A function generator based simulator was used for SNR testing so that external interferences such as movement and physiological noise can be avoided.

The output of the ZenPPG during the experiment was digitized and recorded using the NI DAQ card. Off-line analysis was performed on the acquired data to extract the frequency contents in the 0– to 12-Hz range. The power spectrum of the PPG signals was measured using the Welch method with a Hanning window of 8192 points, and a 50% overlap. The measured frequency spectrum of the input and output signals were normalized to the cardiac component to highlight the noise components. By comparing the input and the output frequency spectrum, the noise components were located. A noise peak with a power greater than the power of the input signal was found at 10 Hz. Fig. 8 shows the frequency spectrum of the input and the output signals in 0-12-Hz range and a

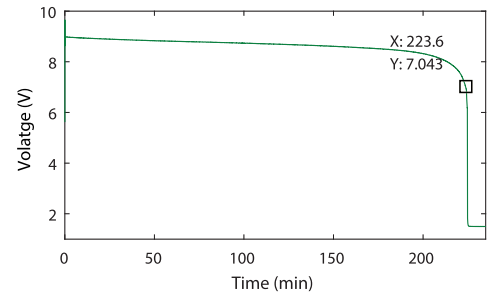


Fig. 9. Changes in battery voltage with time. A steep drop in voltage is observed at 223th min.

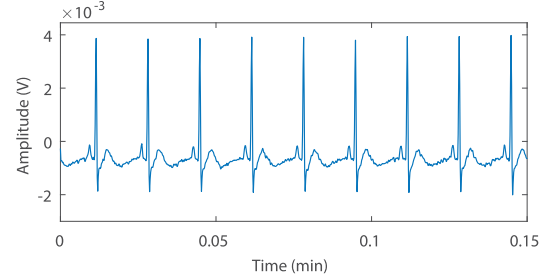


Fig. 10. ECG signal acquired from the ECG amplifier. The ECG leads were attached to a simulator configured to provide a simulated sinus rhythm of 60 beats per minute.

focused view of the noise components at 10 Hz. Since the frequency spectrum is normalized, the power of the noise peak at 10 Hz determines the SNR. Hence, the SNR of the raw PPG signals acquired from the PPG system will be

$$\text{SNR} = 10 \log_{10} \left(\frac{P_{\text{out}}}{P_{\text{in}}} \right) = 50.65 \text{ dB} \quad (2)$$

where P_{out} and P_{in} are the power of the output and input signals.

2) *Power Consumption and Battery Life:* As mentioned earlier, the ZenPPG system works both on batteries and USB power supply. The power consumption of the system, when powered by either power supply, will be the same, and was measured using an ammeter. During the measurement, two commercial pulse oximetry sensors, the ECG cable, thermocouple sensor, and the airway line was connected to the system. The LEDs in each pulse oximetry probe were driven by 40 mA of current. The load current measured by the ammeter was 214 mA. Hence, the power consumption of the system while using batteries is 1.9 W. The test was repeated again by removing the vital sign module so that the power consumption of just the PPG channels can be measured. The load current measured was 176 mA or 1.5 W. From the measured load current, the battery life of the entire system can be calculated and is given as

$$\begin{aligned} \text{Battery life} &= \frac{\text{Battery capacity}}{\text{Load Current}} \times 0.70 \\ &= \frac{1300 \text{ mA}}{214 \text{ mA}} \times 0.7 = 250 \text{ min.} \end{aligned} \quad (3)$$

To verify the calculated result (battery time) experimentally, the changes in the battery voltage were recorded until the

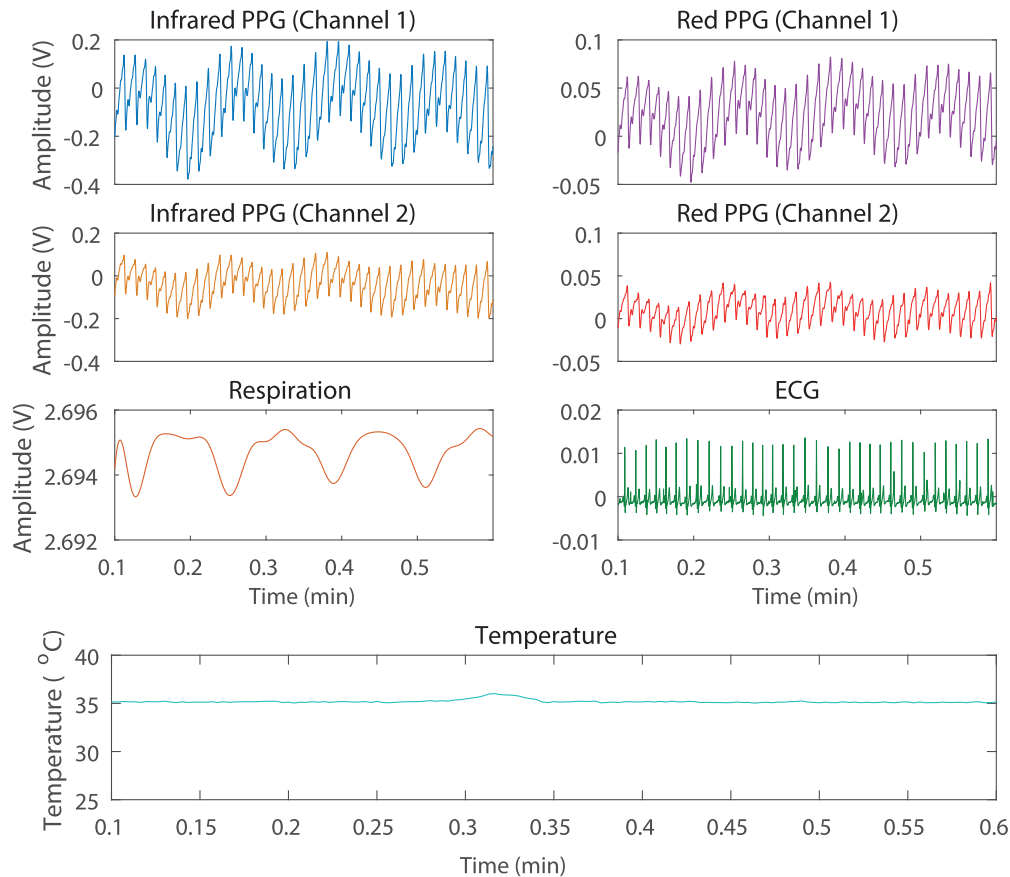


Fig. 11. 30-s snapshot of the infrared and red PPGs acquired from the both the PPG channels of the ZenPPG system along with the respiration, ECG, and temperature signals. The respiration signal is accurately in sync with the amplitude modulation of the PPG signals. The R-wave of the ECG provides the timing reference to the PPG signals.

batteries ran flat, while the system was switched ON and connected to all the sensors. The measurements were recorded using Labview. Fig. 9 shows the results obtained from the battery test. The battery voltage stayed relatively constant for the first 223 mins, after which there was a fast decline in the voltage. The system can, therefore, be used continuously for up to 4 h when powered by batteries.

3) *ECG*: The performance of the ECG amplifier in the vital sign monitoring module was tested using an ECG simulator (ST-20, ECG simulator plus, ST-Electromedicina, Spain). During the experiment, the ECG simulator was connected to the respective leads of the ECG cable (RA, LA, and LL), and an ECG signal with a frequency of 1 Hz (60 BPM) and an amplitude of 0.5 mV was simulated. The output of the ECG amplifier from the ZenPPG system was then recorded using a DAQ card and was stored on laptop PC. Fig. 10 shows the ECG signal acquired from the ECG amplifier. The amplitude of the ECG signal is 14 times the amplitude of the simulated signal, which corresponds to the gain of the instrumentation amplifier.

B. Preliminary Evaluation

Following the technical evaluation, the performance of the developed system was tested *in vivo* on a healthy volunteer.

With the permission of Senate research ethics committee at City, University of London, London, U.K., two Masimo LNCS DCI adult reusable pulse oximeter sensors (Masimo Inc., Irvine, CA, USA) were attached to the index and middle finger of the volunteer. Along with the SpO₂ sensors, the volunteer was connected to a breathing mask, an ECG cable and a K-type thermocouple (on the dorsal surface of the right hand). The red and yellow leads of the ECG cable were connected to the Ag–AgCl easitab ECG electrodes (SKINTACT, F-WA00) placed directly on the right and the left side of the chest and the green (reference) lead connected to the electrode placed on left side of the hip. The two wavelength PPGs, respiration, temperature and ECG signals were recorded using the NI DAQ card (1-kHz sampling frequency) for a period of 5 min, while the volunteer was rested in an armchair. Prior to any analysis the acquired signals were resampled down to 100 Hz using a low-pass (FIR) poly-phase antialiasing filter.

Fig. 11 shows a 30-s snapshot of all the signals acquired from the volunteer. As can be seen from Fig. 11, good quality red and infrared PPGs, ECG, temperature, and respiration data was acquired from the developed system. The respiration signal from the pressure sensor was in sync with the respiration-related amplitude modulations of the AC PPG signals. The capability simultaneous acquisition of all these signals from the ZenPPG system will not only enable the

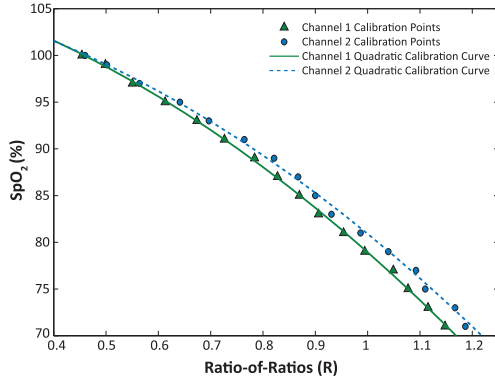


Fig. 12. Calculated R-values of the channel-1 (solid line) and channel-2 (dotted line) plotted against the set SpO_2 values.

estimation of common parameters such as HR, respiration, skin temperature, but will also pave the way to more important parameters such as the arterial oxygen saturation (SpO_2), PTT, PWV, oxygenated and deoxygenated hemoglobin concentrations, HR variability, sympathetic and parasympathetic activity and others.

To demonstrate this ability, both the channels in the ZenPPG system were configured to measure SpO_2 using the commercial pulse oximeter sensors. Since, estimation of SpO_2 requires an empirical calibration curve, both the channels in the ZenPPG system were first calibrated using the Index-2 pulse oximeter simulator (Fluke Biomedical, Washington, USA). This assessment was performed by choosing the preloaded Masimo calibration curve in the simulator and the Masimo reusable finger probe. The pulse oximeter probe was connected to the simulator and SpO_2 values were increased from 70% to 100% with 2% resolution, while the red and infrared PPGs were recorded at each increment for 1 min. The HR was kept constant at 70 beats per minute throughout this process. The R-value (ratio-of-ratio) at each increment was then calculated from the recorded PPGs using the following equation:

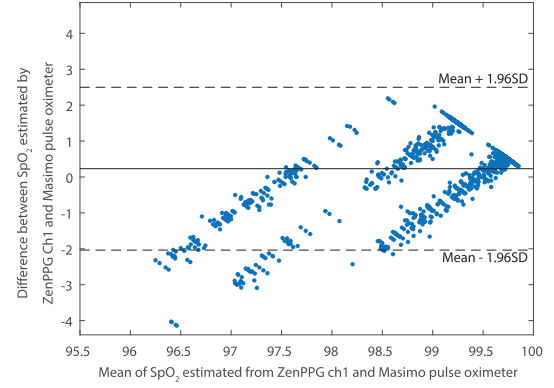
$$R = \frac{\left(\frac{AC_R}{DC_R}\right)}{\left(\frac{AC_{IR}}{DC_{IR}}\right)}. \quad (4)$$

The entire process was repeated again for channel-2, using another Masimo pulse oximeter probe. Fig. 12 shows the calculated R-values from both the ZenPPG channels against the simulated SpO_2 values. A second-degree polynomial was used to derive the following calibration functions from the R-values:

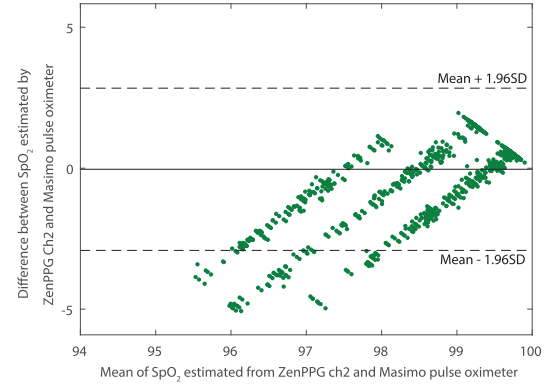
$$\text{SpO}_2 (\text{channel-1}) = -19.49(R^2) - 10.47(R) + 108.9 \quad (5)$$

$$\text{SpO}_2 (\text{channel-2}) = -18.98(R^2) - 7.811(R) + 107.7. \quad (6)$$

Using these calibration curves, the functionality and accuracy of both the ZenPPG channels as pulse oximeters was tested on eight healthy volunteers (aged 21–32). In this brief study, PPG signals were recorded from index and the middle fingers (right hand) of the volunteers using two Masimo reusable sensors (Masimo Inc., California, USA) connected to the ZenPPG system for 2 min. These signals were then used to calculate SpO_2 values, which were compared



(a)



(b)

Fig. 13. Bland Altman plot showing the differences between SpO_2 estimated by (a) Channel-1 and Massimo and (b) Channel-2 and Massimo pulse oximeter.

with simultaneously recorded SpO_2 values from a Masimo Radical-7 commercial pulse oximeter connected to the left index finger of the volunteer. The SpO_2 from both the sensors was calculated by applying 5 and 6 to a 2 s rolling window.

A total of 1592 pairs of SpO_2 values from the eight volunteers (199 values per volunteer) were used to compare each ZenPPG channel with the commercial Masimo pulse oximeter using the Bland and Altman analysis [11]. Fig. 13 shows the differences between SpO_2 estimated by Fig. 13(a) ZenPPG Channel-1 and Massimo and Fig. 13(b) Channel-2 and Masimo pulse oximeter. Calculations of the bias, estimated by the mean difference (d) and the standard deviation of the differences (s) were performed to assess the degree of agreement between each channel of the ZenPPG system with the commercial pulse oximeter. The bias (d) between the channel-1 and the commercial pulse oximeter was $+0.2\%$ with a standard deviation (s) of 1.1% . The bias between channel-2 and the commercial pulse oximeter was -0.03% with a standard deviation of 1.4% . Hence, the limits of agreement for the SpO_2 data

$$\text{Channel 1} = d \pm 1.96 s = 0.2 \pm 1.96 \times 1.1 \quad (7)$$

$$\text{Channel 2} = d \pm 1.96 s = -0.03 \pm 1.96 \times 1.4. \quad (8)$$

IV. DISCUSSION

The unceasing demand for noninvasive and wearable diagnostic tools in the recent years has led researchers to explore the possibility of using PPG as a surrogate tool in an attempt

to measure various hemodynamic parameters, including PTT, hemoglobin concentrations, PWV, and blood pressure. Commercially available technology to acquire PPG signals has for long been restricted to pulse oximeters or patient monitors, which at best, produce one wavelength PPGs that are phase distorted and amplitude modulated. These signals are inadequate to uncover the abundance of information existing within the PPG signals. To ensure continued progress, there is a need for an easily customizable PPG system that produces raw PPG signals and offers an alternative to the integrated solutions with limited adaptability and flexibility such as [24] and [25].

In this paper, we present the design of a novel, modular, and dual-channel PPG research system (ZenPPG) intended for continuous acquisition of undistorted raw dual wavelength PPG signals. The developed system is designed to drive the optical components, detect and sample the two wavelength PPG signals from both channels, and precondition the acquired raw PPG signals. The circuitry required to perform all these tasks was split into four modules which are interconnected via the system bus. Through this modular design approach, various functions in the system were kept independent of each other, which allowed easy debugging, incremental improvements during subsequent development, and easy customization to research needs. For instance, by integrating the vital sign monitoring module into the system, other physiological signals such as the ECG, temperature, and respiration can be acquired on-demand. This ability to acquire raw PPG signals from multiple sites and at multiple wavelengths along with other physiological signals is a distinct advantage over the integrated solutions described for instance in [20]–[25]. Another example of the system's flexibility is the newly developed fiber optic TIA module that connects with traditional PPG sensors and/or fiber optic sensors [29]. These features have allowed the system to be adopted in a wide range of physiological studies investigating hemodynamic changes during mild hypothermia, occlusion, different hand elevations, and head down tilts [30]–[33].

Apart from being modular, the device comprises of many technical features that can potentially impact positively future PPG research. In particular, the independent control over the light intensities of LEDs (resolution <1 mA), and the time multiplexing schema are very useful in *in vivo* studies investigating physiological changes due to interventions. In these studies, predetermined and unaltered light intensities are often required for the entire duration of the study, as automatic changes in light intensity (as in commercial systems) will lead to misinterpretation of the data. The time multiplexing schema implemented in this system also permits dark light sampling, without affecting the sampling time or the multiplexing rates. Furthermore, the architecture of the system allows for acquisition of undistorted raw PPGs from custom-made sensors or from commercial pulse oximeter probes, which is an advantage over commercial systems that connect only to their own probes. This ability will aid the development of PPG sensor technology for monitoring PPGs from locations beyond the finger and the earlobe. Also, the device is made with standard components that are widely available.

The technical evaluations of the ZenPPG system have shown that the system produces good quality raw PPGs, ECGs, temperature and respiration signals. The PPG signals acquired from the system have an SNR of 50.65 dB, and an AC resolution of $150 \mu\text{V}$. The temperature channel has a sensitivity of $10 \text{ mV}/^\circ\text{C}$. The power consumption is also low, the system operates for up to 4 h with two off-the-shelf rechargeable PP3 batteries. As mentioned earlier, the applications of the developed system are also numerous, the preliminary evaluation of the PPG system as a pulse oximeter has produced good results when compared to a commercial pulse oximeter. Although the accuracy of the reported SpO_2 in this brief study is dependent on the calibration function generated from the SpO_2 simulator. The accuracy of the system can be improved by deriving a calibration function through human hypoxic studies. The system has already been used to estimate various other parameter such as PTT [30], oxy and deoxyhemoglobin concentrations [31], HR variability [33], and other PPG morphological parameters [32]. The successive development of the system will be focused on two main aspects. The first will be to implement onboard analog-to-digital conversion and a USB communication protocol so that the use of NI DAQ card is avoided. The other will be to implement a second stage amplifier with DC correction in the TIA module to remove the DC component from the TIA output.

In conclusion, a portable, modular, and multiparametric PPG system was successfully designed and developed to acquire “raw” PPG signals at two wavelengths. It is hoped that this system will help researchers from a wide range of disciplines to customise and integrate this ZenPPG system to their research needs and will enhance research in related fields, particularly in PPG.

REFERENCES

- [1] A. Hertzman and C. Speelman, “Observations on the finger volume pulse recorded photoelectrically,” *Amer. J. Physiol.*, vol. 119, no. 2, pp. 334–335, May 1937.
- [2] A. A. R. Kamal, J. B. Harness, G. Irving, and A. J. Mearns, “Skin photoplethysmography—A review,” *Comput. Methods Programs Biomed.*, vol. 28, no. 4, pp. 257–269, 1989. [Online]. Available: <http://www.sciencedirect.com/science/article/pii/0169260789901594>
- [3] J. G. Webster, *Design of Pulse Oximeters*. Boca Raton, FL, USA: CRC Press, 2002.
- [4] K. Shafqat, R. M. Langford, and P. A. Kyriacou, “Estimation of instantaneous venous blood saturation using the photoplethysmograph waveform,” *Physiol. Meas.*, vol. 36, no. 10, p. 2203, 2015. [Online]. Available: <http://stacks.iop.org/0967-3334/36/i=10/a=2203>
- [5] E. Gil, M. Orini, R. Bailón, J. M. Vergara, L. Mainardi, and P. Laguna, “Photoplethysmography pulse rate variability as a surrogate measurement of heart rate variability during non-stationary conditions,” *Physiol. Meas.*, vol. 31, no. 9, pp. 1271–1290, 2010.
- [6] S. Loukogeorgakis, R. Dawson, N. Phillips, C. N. Martyn, and S. E. Greenwald, “Validation of a device to measure arterial pulse wave velocity by a photoplethysmographic method,” *Physiol. Meas.*, vol. 23, no. 3, p. 581, 2002. [Online]. Available: <http://iopscience.iop.org/0967-3334/23/3/309>
- [7] Y. Yoon, J. H. Cho, and G. Yoon, “Non-constrained blood pressure monitoring using ECG and PPG for personal healthcare,” *J. Med. Syst.*, vol. 33, no. 4, pp. 261–266, Aug. 2009.
- [8] R. P. Smith, J. Argod, J.-L. Pépin, and P. A. Lévy, “Pulse transit time: An appraisal of potential clinical applications,” *Thorax*, vol. 54, no. 5, pp. 452–457, 1999.
- [9] B. M. Pannier, A. P. Avolio, A. Hoeks, G. Mancina, and K. Takazawa, “Methods and devices for measuring arterial compliance in humans,” *Amer. J. Hypertension*, vol. 15, no. 8, pp. 743–753, 2002.

- [10] K. Budidha and P. A. Kyriacou, "The human ear canal: Investigation of its suitability for monitoring photoplethysmographs and arterial oxygen saturation," *Physiol. Meas.*, vol. 35, no. 2, pp. 111–128, Feb. 2014. [Online]. Available: <http://iopscience.iop.org/0967-3334/35/2/111/metrics>
- [11] S. Sathasivam *et al.*, "A novel approach to the assessment of vascular endothelial function," *J. Phys., Conf. Ser.*, vol. 307, no. 1, p. 012014, 2011.
- [12] H. Njoum and P. A. Kyriacou, "Photoplethysmography for the assessment of haemorheology," *Sci. Rep.*, vol. 7, no. 1, 2017, Art. no. 1406.
- [13] P. Kyriacou, S. Powell, R. M. Langford, and D. Jones, "Investigation of oesophageal photoplethysmographic signals and blood oxygen saturation measurements in cardiothoracic surgery patients," *Physiol. Meas.*, vol. 23, no. 3, p. 533, 2002. [Online]. Available: <http://iopscience.iop.org/0967-3334/23/3/305>
- [14] M. Hickey, N. Samuels, N. Randive, R. M. Langford, and P. A. Kyriacou, "Investigation of photoplethysmographic signals and blood oxygen saturation values obtained from human splanchnic organs using a fiber optic sensor," *J. Clin. Monitor. Comput.*, vol. 25, no. 4, pp. 245–255, 2011. [Online]. Available: <http://link.springer.com/article/10.1007/s10877-011-9302-4>
- [15] J. P. Phillips, R. M. Langford, S. H. Chang, K. Maney, P. A. Kyriacou, and D. P. Jones, "Cerebral arterial oxygen saturation measurements using a fiber-optic pulse oximeter," *Neurocritical Care*, vol. 13, no. 2, pp. 278–285, Oct. 2010. [Online]. Available: <http://dx.doi.org/10.1007/s12028-010-9349-y>
- [16] B. C. Stack, Jr., N. D. Futran, B. Zang, and J. E. Scharf, "Initial experience with personal digital assistant-based reflectance photoplethysmograph for free tissue transfer monitoring," *Ann. Plastic Surg.*, vol. 51, no. 2, pp. 136–140, 2003.
- [17] S. S. Thomas *et al.*, "BioWatch—A wrist watch based signal acquisition system for physiological signals including blood pressure," in *Proc. 36th Annu. Int. Conf. IEEE Eng. Med. Biol. Soc. (EMBC)*, Aug. 2014, pp. 2286–2289.
- [18] R. Rawassizadeh, B. A. Price, and M. Petre, "Wearables: Has the age of smartwatches finally arrived?" *Commun. ACM*, vol. 58, no. 1, pp. 45–47, 2015.
- [19] V. Rybnyok, J. M. May, K. Budidha, and P. Kyriacou, "Design and development of a novel multi-channel photoplethysmographic research system," in *Proc. IEEE Point-Care Healthcare Technol. (PHT)*, Jan. 2013, pp. 267–270.
- [20] A. Tobola *et al.*, "Self-powered multiparameter health sensor," *IEEE J. Biomed. Health Inform.*, vol. 22, no. 1, pp. 15–22, Jan. 2018.
- [21] M. Konijnenburg *et al.*, "A multi(bio)sensor acquisition system with integrated processor, power management, 8×8 LED drivers, and simultaneously synchronized ECG, BIO-Z, GSR, and two PPG read-outs," *IEEE J. Solid-State Circuits*, vol. 51, no. 11, pp. 2584–2595, Nov. 2016.
- [22] P.-F. Rüedi *et al.*, "Ultra low power microelectronics for wearable and medical devices," in *Proc. IEEE Design, Autom. Test Eur. Conf. Exhibit. (DATE)*, Mar. 2017, pp. 1426–1431.
- [23] M. G. Srinivasa and P. S. Pandian, "Wireless wearable remote physiological signals monitoring system," in *Proc. Int. Conf. Circuits, Controls, Commun. Comput. (I4C)*, Oct. 2016, pp. 1–5.
- [24] Texas Instruments. (2014). *Afe4490—Integrated Analog Front-End for Pulse Oximeters*. [Online]. Available: <http://www.ti.com/lit/ds/symlink/afe4490.pdf>
- [25] Maxim Integrated. (2014) *Max30100—Pulse Oximeter and HeartRate Sensor IC for Wearable Health*. [Online]. Available: <https://datasheets.maximintegrated.com/en/ds/MAX30100.pdf>
- [26] J. G. Graeme, *Amplifier Applications of Op Amps*, vol. 1. New York, NY, USA: McGraw-Hill, 1999.
- [27] *Sample-and-Hold Amplifiers, Analog Devices Tutorials*, Analog Devices, Norwood, MA, USA, Oct. 2008, p. 21.
- [28] K. Budidha, "In vivo investigations of photoplethysmographs and arterial oxygen saturation from the auditory canal in conditions of compromised peripheral perfusion," Ph.D. dissertation, Res. Centre Biomed. Eng., School Math., Comput. Sci. Eng., Univ. London, London, U.K., 2016. [Online]. Available: <http://ethos.bl.uk/OrderDetails.do?uin=uk.bl.ethos.702030>
- [29] J. J. Davenport, M. Hickey, J. P. Phillips, and P. A. Kyriacou, "Fiber-optic fluorescence-quenching oxygen partial pressure sensor using platinum octaethylporphyrin," *Appl. Opt.*, vol. 55, no. 21, pp. 5603–5609, 2016.
- [30] K. Budidha and P. A. Kyriacou, "Investigation of pulse transit times utilizing multisite reflectance photoplethysmography under conditions of artificially induced peripheral vasoconstriction," in *Proc. 36th Annu. Int. Conf. IEEE Eng. Med. Biol. Soc. (EMBC)*, Chicago, IL, USA, Aug. 2014, pp. 1965–1968.
- [31] T. Y. Abay and P. A. Kyriacou, "Reflectance photoplethysmography as noninvasive monitoring of tissue blood perfusion," *IEEE Trans. Biomed. Eng.*, vol. 62, no. 9, pp. 2187–2195, Sep. 2015.
- [32] M. Hickey, J. P. Phillips, and P. Kyriacou, "The effect of vascular changes on the photoplethysmographic signal at different hand elevations," *Physiol. Meas.*, vol. 36, no. 3, p. 425, 2015.
- [33] M. C. Hemon and J. P. Phillips, "Comparison of foot finding methods for deriving instantaneous pulse rates from photoplethysmographic signals," *J. Clin. Monitor. Comput.*, vol. 30, no. 2, pp. 157–168, Apr. 2016.



Karthik Budidha received the B.Eng. degree in biomedical engineering from City, University of London, London, U.K., in 2009, the M.Sc. degree in biomedical engineering and medical physics from Imperial College London, London, U.K., in 2010, and the Ph.D. degree in biomedical engineering, City, University of London, in 2016.

He was with Hillingdon Hospital, Uxbridge, UK., as a Biomedical Engineer. He is currently a Post-Doctoral Research Associate with the Research Centre for Biomedical Engineering, City, University of London. His current research interests include in the design of novel optical sensors, and the development of bio-electronic instrumentation to continuously monitor physiological and behavioural variables for early diagnosis of cardiovascular diseases.



Victor Rybnyok received a higher education diploma degree in computer systems and networks engineering from the Moscow Institute of Electronic Technology, Moskva, Russia, in 2001, the M.Sc. degree in medical electronics & physics from Queen Mary, University of London, London, U.K., in 2003, and the Ph.D. degree in biomedical engineering from City University London, in 2009.

He was with Biomedical Engineering Research Group in City University London on personal health care software and bio-optics theory and instrumentation projects. He is currently a Software Research and Development Engineer on the embedded web server user interface for distributed sensors network with real-time signal processing, data acquisition, visualisation, and instrumentation control.



Panayiotis A. Kyriacou (SM'06) received the B.E.Sc. degree in electrical engineering from the University of Western Ontario, London, ON, Canada, and the M.Sc. and Ph.D. degrees in medical electronics and physics from St. Bartholomew's Medical College, University of London, London, U.K.

He is currently a Professor of biomedical engineering and the Associate Dean for Research and Enterprise with the School of Mathematics Computer Science and Engineering, City University London. He is also the Director of the Research Centre for Biomedical. His current research interests include the understanding, development, and applications of medical instrumentation and sensors to facilitate the prognosis, diagnosis, and treatment of a disease or the rehabilitation of patients.

Dr. Kyriacou served as the Chair of the Physiological Measurement Group, the Engineering Advisory Group at the Institute of Physics and Engineering in Medicine (IPEM), and the Instrument Science and Technology Group of the Institute of Physics. He is also an Adjunct Professor at Yale Medical School, Honorary Professor at the Indian Institute of Technology Roorkee, Roorkee, India, and an Honorary Senior Research Fellow at Great Ormond Street Hospital for Children and St. Bartholomew's Hospital, W Smithfield, London, U.K. He is currently the Vice President Academia at IPEM and the president of the European Alliance for Medical and Biological Engineering & Science.